Available online at www.sciencedirect.com
ScienceDirect
Ceramics International 37 (2011) 715–723
CERAMICS INTERNATIONAL
www.elsevier.com/locate/ceramint

Phase evolution during the low temperature formation of stoichiometric hydroxyapatite-gypsum composites

Yaser E. Greish *

Department of Chemistry, College of Science, United Arab Emirates University, Al Ain, United Arab Emirates

Received 1 July 2010; received in revised form 9 August 2010; accepted 26 September 2010
Available online 29 October 2010

Abstract

Both plaster of Paris ($CaSO_4 \cdot (1/2)H_2O$, POP) and bone-like synthetic calcium phosphates (CaP) have been used as bone-like cements. The current study investigated the formation of composites involving POP with each of three types of stoichiometric hydroxyapatites (abbreviated as SHAp, S-SH, and C-SH, each with a Ca/P molar ratio of 1.67). The kinetics, variations in solution chemistry during the formation of these composites and phase compositions of the formed products were investigated over a course of 24 h. Although the presence of gypsum precursors was shown to decrease the alkalinity of the medium involving SHAp formation from its precursors, a delay in the growth kinetics of gypsum was observed. The same behavior was observed in the presence of commercial apatite (C-SH), whereas in the presence of synthetic apatite (S-SH), no delay was observed. A possibility of formation of a calcium sulfate phosphate double salt, as an intermediate, was investigated and confirmed by XRD analysis.

Keywords: Gypsum; Stoichiometric hydroxyapatite; Isothermal calorimetry; Phase composition; Microstructure

1. Introduction

Calcium phosphate cements have been extensively studied because of the convenience and ease of preparation compared to calcium phosphate bioceramics prepared at high temperatures. These cements are injectable and consolidate inside bone in a form of bone-like apatite [1]. They are ideal as reconstructive materials for bone defects, they fit in well, harden *in situ*, and are replaced by osseous tissue [2].

Calcium hydroxyapatite can be produced at physiological temperature from an aqueous slurry of calcium phosphate precursors [3] or by the hydrolysis of a single phosphate salt [4]. Both routes lead to the formation of a monolithic bone-like apatite. However, preparations in which apatite forms by the hydration of α-tricalcium phosphate (α-$Ca_3(PO_4)_2$) as a single phase with solution may require lengthy periods for complete reaction to occur [4]. This may not be problematic, for it results in uncertainty with regard to longer term variations in chemistry which may be cytotoxic. More importantly, predicting property development becomes more difficult if the healing process has initiated before reactions leading to HAp are complete. On the other hand, formulations involving tetracalcium phosphate ($Ca_4(PO_4)_2O$), and dicalcium phosphate ($CaHPO_4 \cdot 2H_2O$) as apatite precursors have proven to possess better kinetics of apatite formation [5]. Moreover, they have been shown to provide the possibility of controlling the calcium deficiency in the produced apatite [5].

Calcium sulfate is a highly biocompatible material that is one of the simplest synthetic bone graft materials with the longest clinical history, spanning more than 100 years [6]. Calcium sulfate has been successfully used to treat periodontal disease, endodontic lesions, alveolar bone loss, and maxillary sinus augmentation [6]. It can be used as a binder, facilitating healing and preventing loss of the grafting material. Moreover, it is tissue compatible, and does not interfere with the healing process [7]. POP was previously shown to improve the setting reactions of a biodegradable calcium phosphate cement that was composed of β-tricalcium phosphate (β-$Ca_3(PO_4)_2$) and monocalcium phosphate monohydrate ($Ca(H_2PO_4)_2 \cdot H_2O$) [8]. Due to their chemical composition and porous structure, these cements are resorbable and osteoconductive [8].

* Corresponding author. Permanent address: Department of Ceramics, National Research Center, Cairo, Egypt. Tel.: +971 50 233 8203; fax: +971 3 767 1291.
E-mail address: y.afifi@uaeu.ac.ae.

0272-8842/$36.00 © 2010 Published by Elsevier Ltd and Techna Group S.r.l.
doi:10.1016/j.ceramint.2010.09.046

POP-based biomaterials have also exhibited promise as grafts in a preclinical repair model of intrabony periodontal defects, as well as in clinical reports for sinus augmentation and treatments of femoral shaft nonunions [9–11]. Moreover, POP was used to modulate the setting time, workability and porosity of a cement composed of an aqueous slurry of α-$Ca_3(PO_4)_2$ [12–14]. Nilsson et al. [13] further summarized the major role of gypsum when mixed with α-TCP in the creation of pores in the implanted material, thus ensuring ingrowth of new bone tissue. Sato et al. further indicated the promising characteristics of gypsum after mixing it with HAp particles, based on the relatively fast absorption of gypsum without interfering with the process of bone healing [15]. In an attempt to use gypsum as a bone graft substitute for lumbar spinal fusion, CSD showed unsuccessful results because of its rapid resorption [16].

The proposed formulation is based on a tetracalcium phosphate-dicalcium phosphate cement system with a POP added as a modulator of the hydraulic activity and hence the mechanical properties of the produced cements. By varying the proportions of the reactants, cements with different degrees of biodegradation are expected to form. A preliminary set of experiments proved the dependence of the biodegradability of the produced composite on the concentration of POP [17]. According to the author's knowledge, this proposed system is novel and carries a lot of expectations for a wide range of orthopedic and dental applications.

2. Materials and methods

Three types of stoichiometric hydroxyapatite, with Ca/P molar ratio of 1.67, were used in the current study. A commercial hydroxyapatite, abbreviated hereafter as C-SH, was obtained from Sigma–Aldrich, USA as fine powder with an average particle size of 3 μm, as determined by scanning electron microscopy. A synthetic hydroxyapatite, abbreviated hereafter as S-SH, was prepared using a common wet method. A 0.3 M aqueous solution of $NH_4H_2PO_4$ (obtained from Sigma–Aldrich, USA) was added to a 0.5 M aqueous solution of $Ca(NO_3)_2{\cdot}4H_2O$ (obtained from Sigma–Aldrich, USA) under constant temperature of 70 °C and vigorous stirring. pH of the suspension was adjusted at 10–11 using an aqueous ammonia solution. S-SH precipitate was separated from its suspension by filtration, washed with de-ionized water then dried at 100 °C for 24 h. Dried powders were further calcined at 800 °C for 1 h, then finely ground. The ground particles were not agglomerated and were found to have an average particle size of 4 μm, as determined by scanning electron microscopy.

The third type of stoichiometric hydroxyapatite used, abbreviated hereafter as SHAp, was prepared *in situ* using an acid–base reaction between tetracalcium phosphate ($Ca_4(PO_4)_2O$; TetCP) and anhydrous dicalcium phosphate ($CaHPO_4$; DCPA). TetCP was prepared via heating a powder mixture comprising $CaCO_3$ (Osram Sylvania, USA) and monocalcium phosphate monohydrate ($Ca(H_2PO_4)_2{\cdot}H_2O$; MCPM) (Sigma, USA) with a molar ratio of 3:1, at 1310 °C for 2 h in air. Phase-pure TetCP powder, as confirmed by X-ray diffraction, was attrition milled to a particle size of 2.5 μm. SHAp precursors mixture was prepared by a mechanochemical process where a powder mixture of TetCP and MCPM, at a Ca/P ratio of 1.67, was milled in n-Heptane. Previous results showed that this process yielded an intimate mixture of TetCP and DCPA, according to reaction (1) [5]:

$$2Ca(H_2PO_4)_2{\cdot}H_2O + 7Ca_4(PO_4)_2O \rightarrow 6CaHPO_4 + 6Ca_4(PO_4)_2O + 3H_2O \quad (1)$$

This intimate mixture is known to form SHAp when mixed with de-ionized water at a power-to-liquid ratio of 2 [5]. Analytical grade plaster of Paris ($CaSO_4{\cdot}(1/2)H_2O$, POP) was obtained from Sigma–Aldrich, USA, and was used as purchased. Analytical grade gypsum ($CaSO_4{\cdot}2H_2O$, G), also obtained from Sigma–Aldrich, USA, was used for comparison during the characterization of the reaction products.

Powder mixtures of each of the three types of stoichiometric hydroxyapatites were formed by mixing them with POP in weight percentage of 10, 25, 50, and 75 of the apatite. Details of these mixtures and the corresponding samples designations are given in Table 1.

Pure samples of POP and SHAp precursors were used for comparison. An exact weight of 3 g of each of the powder mixtures was mixed with de-ionized water at a powder:liquid ratio of 2:1 by weight. Heat evolution during the conversion of POP into gypsum in the presence of different proportions of each of the three apatites, was recorded for 24 h using an isothermal calorimetry (IC) technique (Thermometrics Corp., San Diego, CA, USA), as described by Prosen et al. [18]. Aqueous suspensions of each of these mixtures were also formed at a powder-to-liquid ratio of 0.01 to study the variations in their pH with time, for up to 24 h, as a result of conversion of POP into gypsum in the presence of each of the

Table 1
Details of the starting mixtures and their corresponding samples designations.

Sample details	Ca/P	Method of preparation	Sample designation			
			10%	25%	50%	75%
Pure gypsum	N/A	Cement-type	G100			
Stoichiometric HAp	1.67	Cement-type	SHAp10	SHAp 25	SHAp 50	SHAp 75
Synthetic stoichiometric HAp		Wet method	S-SH10	S-SH25	S-SH50	S-SH75
Commercial HAp		Wet method[a]	C-SH10	C-SH25	C-SH50	C-SH75

[a] As mentioned in the technical data sheets provided with the product from.

apatitic precursors. A calibrated pH electrode interfaced to an Orion 920 pH meter was used in this regard, where each of the powder/water mixtures was placed in a double-walled glass beaker equilibrated at 37.4 °C. At the end of each experiment, the slurry was filtered and the separated solids were flushed with acetone to stop further reaction. After drying, phase composition of each of the filtered solid residues was investigated by X-ray diffraction (XRD) and infrared spectroscopy (IR) techniques. During each of these experiments, solids were also separated from the suspensions at certain time periods, decided by the IC and pH results, for further analysis by XRD. An automated X-ray diffractometer, with a step size of 0.02°, scan rate of 2° per min, and a scan range from $2\theta = 20°$–40° was used. A Nicolet Nexus 470 infrared (IR) spectrophotometer infrared spectroscopy (IR), USA was used where samples, pre-pressed with KBr, were scanned over the normal range of 4000–400 cm^{-1}. Selected dry solid samples were evaluated for their microstructure using a JEOL SEM at an accelerating voltage of 15 kV.

3. Results and discussion

It was previously found that when DCPA and TetCP were proportioned to produce SHAp, the pH of the solution migrated toward that of the invariant point between SHAp and $Ca(OH)_2$ [18]. Complete deposition of stoichiometric hydroxyapatite took place in around 3 h, which is thought to be clinically relevant. However, the elevated pH was inconsistent with clinical applications [19]. Fig. 1 shows the variations in the pH during the concurrent formation of SHAp and gypsum phases. In the absence of gypsum precursors, pure SHAp precursors mixture showed an increase in the pH of the medium achieving a pH of 10.8 as its highest point after around 6 h. This indicates that the dissolution of the SHAp precursors is dominated by TetCP, the basic component of this system [5,20]. Dissolution of TetCP and DCPA starts with the first contact with water where a sudden increase in the pH of the medium

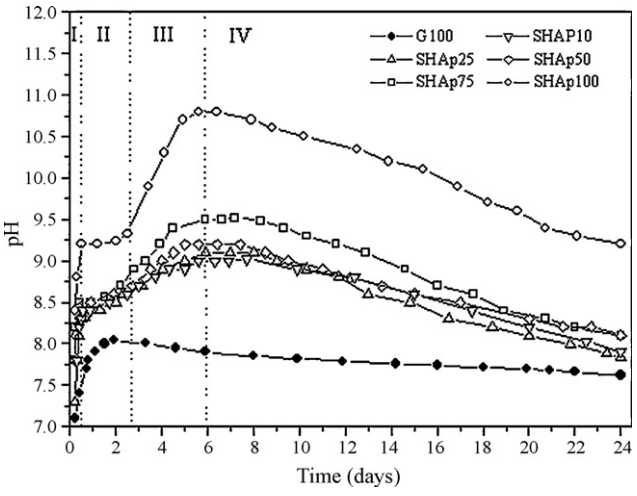

Fig. 1. Variation in pH of suspensions containing gypsum and SHAp precursors at weight percentages of 10, 25, 50 and 75 of the later, hydrated for 24 h at 37.4 °C. Pure SHAp100 and G100 are shown for comparison.

took place to a pH of 9.25 within the first 30 min, region I in Fig. 1. This increase is due to the dissolution of TetCP and DCPA, although dominated by the first phase. An intermediate Ca-deficient HAp, with an average composition of $Ca_{(10-x)}(HPO_4)_x(PO_4)_{(6-x)}(OH)_{(2-x)}$, $0 < x < 1$, was previously found to form [5,20]. Region II in Fig. 1 shows a steady state, lasting for 2 h, where the formation of this intermediate phase and the dissolution of the remaining DCPA took place. Once the DCP has been consumed; by the end of region II, continued hydrolysis of TetCP is shown to result in pH elevation, as shown in region III of Fig. 1, up to a pH value of 10.8. Ca-deficient HAp will convert to stoichiometric HAp under these conditions. The onset of HAp precipitation via the incorporation of calcium ions, liberated during conversion of TetCP to HAp, into the structure of the pre-existing Ca-deficient HAp will reduce the pH; region IV in Fig. 1.

On the other hand, dissolution of POP and its conversion to gypsum, in the absence of SHAp precursors, is also shown in Fig. 1 to take place through two steps. The first step is represented by a sudden increase in the pH of the medium, achieving a maximum value of 8.1 after 2 h. This is attributed to the first stage of POP conversion to gypsum which involves the dissolution of POP and the liberation of Ca^{2+} and SO_4^{2-} ions into the medium, causing the medium pH to increase. This step is followed by a slow decrease in the pH of the medium as a result of gypsum deposition, achieving a minimum pH value of 7.7 after 24 h. The slow decrease in the pH of the medium indicates the slow conversion of POP into gypsum. The presence of POP, at different proportions, within the SHAp initial powder mixture caused a decrease in the alkalinity of the solution that was first attributed to the dissolution of TetCP. The maximum pH values achieved in these composites were 9.5, 9.2, 9.1, and 9.0 in the presence of 75, 50, 25, and 10 wt% of SHAp precursors, respectively. In the co-existence of SHAp and gypsum precursors, it is apparent that their dissolution patterns took place in a manner similar to that of pure SHAp system. These findings together with the relatively alkaline pH values reached in these mixtures indicate that the dissolution of these precursors is dominated by TetCP, the most basic component in the existing mixtures.

Heat evolution during the formation of SHAp from its precursors was previously studied by isothermal calorimetry [21]. Using this technique, heat of formation of different compounds was determined. Normally, three peaks related to the different stages resulting in the formation of the final products, are observed. During the formation of SHAp; curve S100 in Fig. 2, these three peaks can be seen. These are related to the wetting/dissolution of the solid precursors, followed by nucleation of the new product seeds, and finally end with the growth of these seeds into the crystalline final product; SHAp. As shown in Fig. 2, the wetting/dissolution and the nucleation peaks took place during the first 30 min of reaction. Following these initial stages, a growth peak spanning over 7 h is observed in Fig. 2. Formation of SHAp from TetCP and DCPA precursors is known to take place through a dissolution–precipitation process, where DCPA starts dissolving, followed by TetCP. As a result of this step, the surrounding aqueous

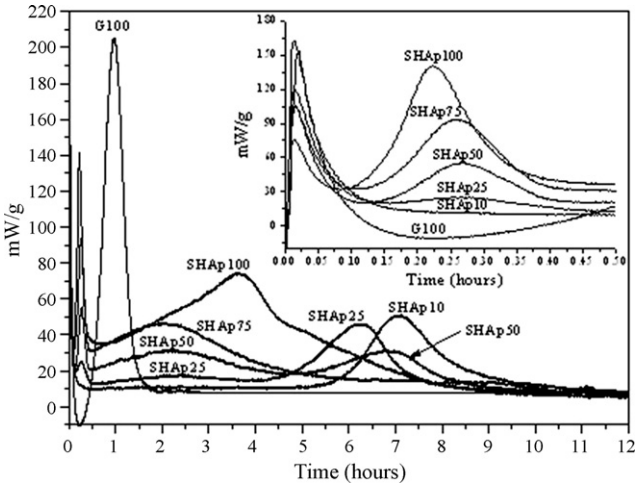

Fig. 2. Calorimetric curves indicating evolution of heat in composites containing gypsum and SHAp precursors at weight percentages of 10, 25, 50 and 75 of the later, as a result of their hydration at 37.4 °C for 12 h. Pure SHAp100 and G100 are shown for comparison (insert: details of the wetting/initial dissolution peak in all composites within the first 30 min).

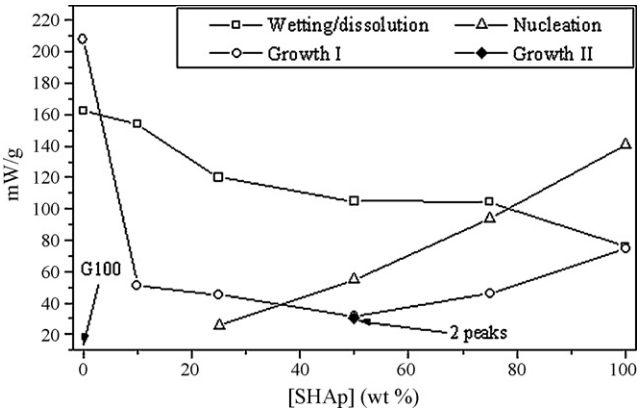

Fig. 3. Variation in the heat evolved during the different stages of hydration of composites containing gypsum and SHAp precursors at weight percentages of 10, 25, 50 and 75 of the later, at 37.4 °C for 18 h.

medium becomes supersaturated with respect HAp, leading to precipitation of the later, as shown in reaction (2).

$$2Ca_4(PO_4)_2O + 2CaHPO_4 \rightarrow Ca_{10}(PO_4)_6(OH)_2 \quad (2)$$

In contrast, the process of formation of gypsum from its POP precursor is reflected in two peaks only, as shown in Fig. 2. These peaks represent the wetting/dissolution and the nucleation/growth, where a rapid growth takes place concurrent with the nucleation giving rise to a single peak representing both steps. Similar to SHAp, wetting/dissolution process took place during the first 30 min, while the nucleation/growth combined process spanned for 1 h only, ceasing in 1.5 h from the beginning of mixing. The absence of a nucleation peak during the deposition of gypsum out of the solution is clearly represented in the insert of Fig. 1. Reaction (3) illustrates the conversion of POP into gypsum:

$$CaSO_4 \cdot \tfrac{1}{2}H_2O + 1\tfrac{1}{2}H_2O \rightarrow CaSO_4 \cdot 2H_2O \quad (3)$$

Similar to the pure gypsum system, Fig. 2 indicates that a nucleation peak was neither present in the cement mixture containing 10 wt% of SHAp precursors. On the other hand, the presence of POP precursors was observed to slightly delay the time of the nucleation peak where nucleation peaks of composites containing 25, 50, and 75 wt% SHAp precursors peaked at 0.26, 0.27, and 0.28 h, respectively compared to 0.2 h for pure SHAp sample.

Growth peaks of the SHAp-gypsum precursors mixtures are shown in Fig. 2, while their peak values are summarized in Fig. 3. In the presence of 10 wt% SHAp precursors, a single growth peak was observed after 7 h of mixing. Despite the fact that this mixture contained a majority of 90 wt% gypsum precursors, a delay of 6 h of the growth peak was observed, compared to that of pure Gypsum. This delay could be attributed to the absence of a nucleation peak; see the insert of Fig. 2. Despite this delay, the presence of this growth peak indicates the slow formation of nuclei without releasing heat, and the consequent growth of these nuclei when their concentration was high enough to initiate the growth. These observations were confirmed with composite mixtures containing 25 wt% SHAp precursors where a growth peak was observed after 6.2 h of mixing. The appearance of this growth peak at a relatively earlier time compared to that of S10 sample could be attributed to the presence of a weak nucleation peak for S25 sample after 15 min of mixing. Composite mixture containing 50 wt% SHAp precursors was the only mixture to show two growth peaks; after 2 and 7 h. Formation of SHAp and gypsum products through hydration of their precursors is known to take place through a dissolution–precipitation mechanism in which reactants partially dissolve, release ions into solution, which in turn re-precipitate in the form of the final product. In the presence of each other, it seems that the mechanism of formation of each of them is affected by the presence of precursors of the other phase. In the presence of a majority of 75 wt% SHAp precursors, only one growth peak was observed after 2 h of mixing, similar to that of 100% SHAp where a single growth peak appeared after 3.5 h of mixing. In all composite mixtures, the rapid growth of gypsum, that was observed as a single peak in 100% pure gypsum sample, was not observed in the tested mixtures.

In contrast to the co-setting of gypsum and SHAp precursors, the conversion of POP into gypsum in the presence of a commercially available HAp (C-SH) was also studied by isothermal calorimetry. Fig. 4A shows the IC curves obtained in this regard. Solubility of C-SH is known to be very limited; with a K_{sp} value of around 1×10^{-36}. As was previously shown in Fig. 2, two peaks were observed in the IC curves of these powder mixtures; wetting/dissolution and growth peaks. Intensity of the growth peak was shown to decrease by increasing the proportion of the relatively less reactive reactant; C-SH. A slight shift in the position of the peak maxima was observed from 1 h for pure gypsum to 1.4 and 1.7 h for mixtures containing 50 and 75% by weight of C-SH, respectively. This was initially accompanied by relatively higher wetting/dissolution than those of pure gypsum and gypsum composites

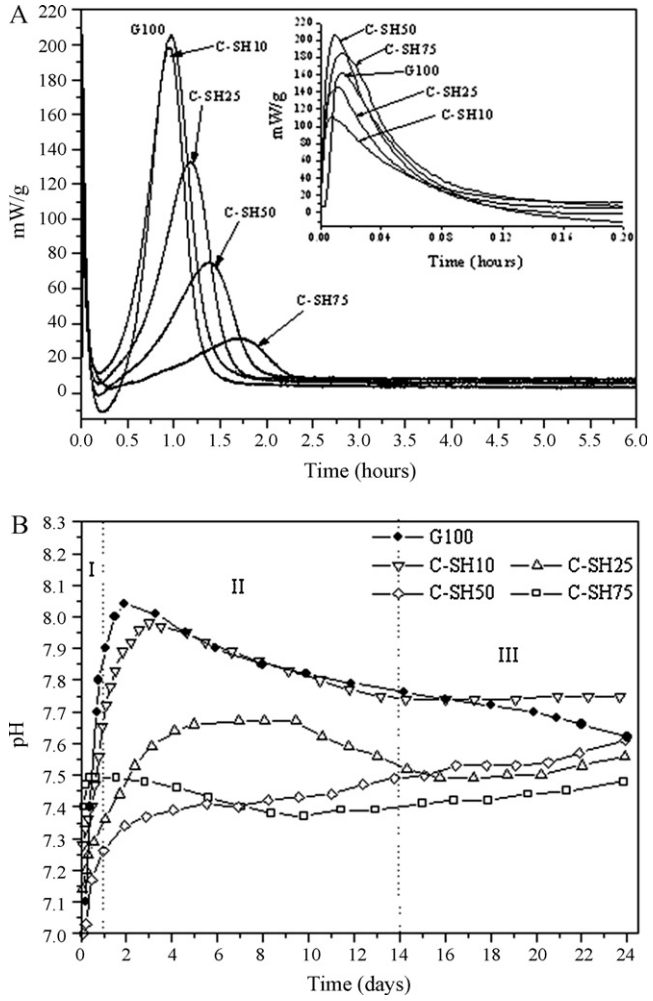

Fig. 4. (A) Calorimetric curves indicating evolution of heat in composites containing gypsum precursors and C-SH powders at weight percentages of 10, 25, 50 and 75 of the later as a result of their hydration at 37.4 °C for 6 h. Pure G100 is shown for comparison (insert: details of the wetting/initial dissolution peak in all composites within the first 15 min). (B) Variation in pH of suspensions containing gypsum precursors and C-SH powders at weight percentages of 10, 25, 50 and 75 of the later, hydrated for 24 h at 37.4 °C. Pure G100 is shown for comparison.

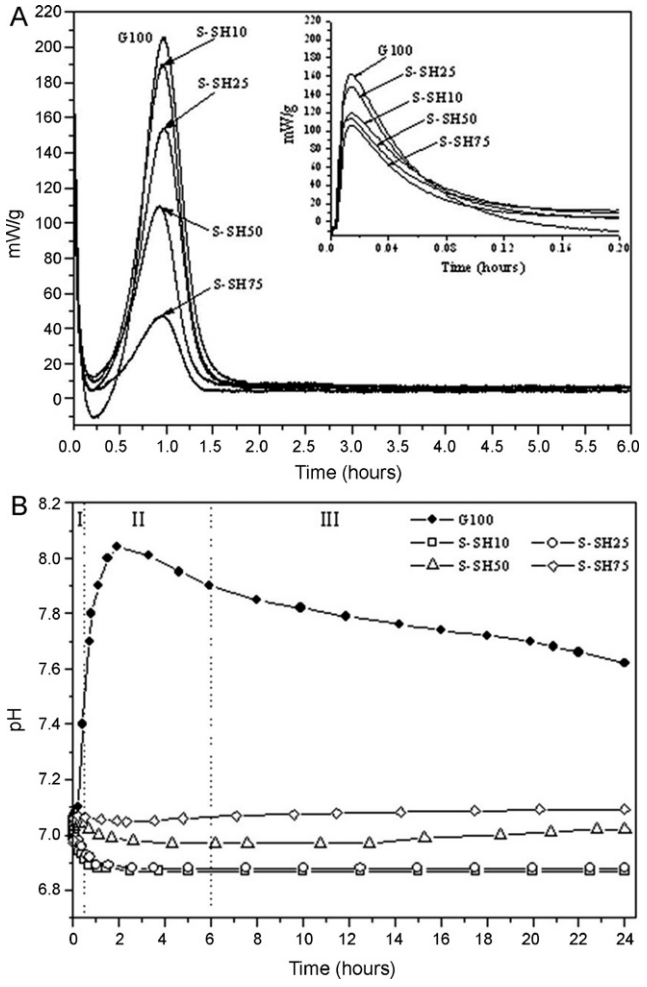

Fig. 5. (A) Calorimetric curves indicating evolution of heat in composites containing gypsum precursors and S-SH powders at weight percentages of 10, 25, 50 and 75 of the later as a result of their hydration at 37.4 °C for 6 h. Pure G100 is shown for comparison (insert: details of the wetting/initial dissolution peak in all composites within the first 15 min). (B) Variation in pH of suspensions containing gypsum precursors and S-SH powders at weight percentages of 10, 25, 50 and 75 of the later, hydrated for 24 h at 37.4 °C. Pure G100 is shown for comparison.

with 10 and 25 wt% C-SH. Gypsum was formed in all composites after 2 h of mixing, while C-H remained unchanged. Variations in the pH of the solutions containing POP/C-SH powder mixtures are shown in Fig. 4B. A decrease in the overall pH regime of the studied suspensions is shown to take place consistently with increasing the proportion of C-SH in these mixtures. This could be solely attributed to the decrease in the concentration of POP from which Ca^{2+} and SO_4^{2-} ions are liberated and cause the changes in the pH of the medium. Despite the slight delay in the deposition of gypsum, shown in Fig. 4A, it should be mentioned in this regard that the addition of C-SH has buffered the system achieving a physiologic pH range of 7.3–7.6.

In the presence of synthetic HAp (S-SH), a decrease in the intensity of both dissolution/wetting and growth peaks was observed in all composites compared to pure gypsum samples; Fig. 5A. This decrease seems to be proportional to the decrease in the concentration of POP in the starting powder mixture. No delay was observed in growth peak of gypsum, ending in all composites in 1.5 h. These composites contain ready-made stoichiometric HAp, which is expected to have the same relative inactivity as that of C-SH. However, the observed delay in the growth peak of gypsum in Fig. 4B indicates the slight contribution of C-SH in the conversion of POP into gypsum. Although this delay was not so pronounced as that observed in Fig. 2, this could be attributed to the possibility of presence of non-stoichiometric HAp impurities in the C-SH powder used. This is also evident in the pH curves of composites containing C-SH in Fig. 4B, where composites containing 50 wt% of C-SH showed a peak value at 7.4, followed in both cases by slow increase in their pH achieving a maximum of 7.6 after 24 h. On the other hand, composites containing 75 wt% of C-SH showed a peak at 7.49 followed by a decrease down to 7.37 after 10 h then a slight increase to 7.48 after 24 h. In contrast, the pH

curves in Fig. 5B show an overall buffering effect with an overall steady pH range of 6.9–7.1. Despite the fact that S-SH was not evident to participate in the conversion of POP into gypsum, the overall decrease in the pH regime of composites containing S-SH could be mainly attributed to the decrease in the concentration of POP in the original powder mixtures. Taken together, these findings support the idea that the co-formation of SHAp and gypsum, shown in Fig. 2, was highly affected by the dissolution of calcium ions from their precursors.

A study of the phase composition of these mixtures was carried out using XRD for precipitates taken out of the medium after 6 and 24 h of mixing for composites containing 50 wt% of SHAp precursors. This was based on the fact that this mixture previously showed two growth peaks in the IC curves in Fig. 2. XRD results are shown in Fig. 6. XRD patterns were further compared to those of the standard samples; 25-1137, 9-432 and 9-80 for standard TetCP, HAp, and DCPA, respectively. XRD patterns of pure POP and Gypsum samples were also shown. In addition XRD patterns of two new combined salts are shown. Those are 41-585 for calcium phosphate sulfate hydroxide hydrate ($Ca_2(SO_4)(HPO_4)\cdot 4H_2O$; Ardealite) and 46-657 for calcium phosphate sulfate hydrate ($Ca(HPO_4)_x(SO_4)_{1-x}\cdot 2H_2O$). Compared to a complete conversion of POP into gypsum in less than 2 h; end of growth peak of pure gypsum, there was no sign of gypsum in the XRD patterns of the solid mixture of S50 after 6 h. In contrast, gypsum dominated the XRD patterns of these composites after 24 h with SHAp as the second phase with a concentration that increased with increasing the original concentration of its precursors in the original powder mixtures.

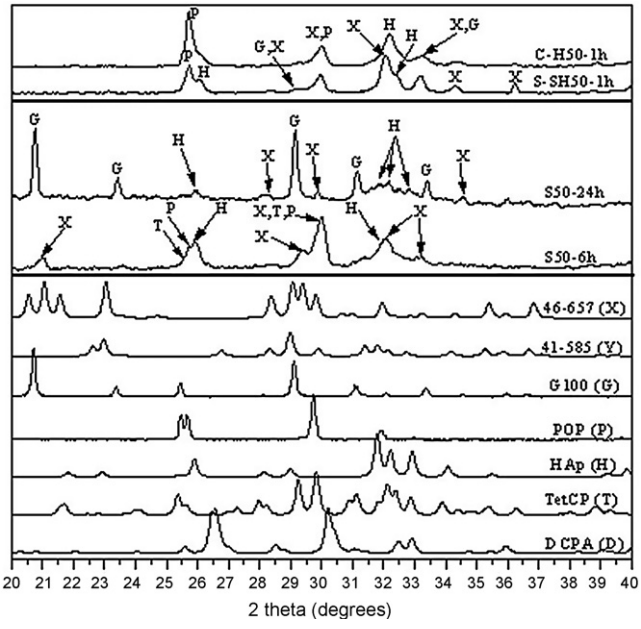

Fig. 6. XRD patterns of composite powders containing 50 wt% of SHAp with gypsum after hydration in de-ionized water for 6 and 24 h at 37.4 °C. Patterns of composites containing 50 wt% of S-SH and C-SH with gypsum after hydration in de-ionized water for 1 h are also shown. XRD pattern of pure POP and G100 samples are shown for comparison. Patterns of standard HAp, TetCP, DCPA and two calcium sulfate phosphate phases are also shown for comparison.

Un-reacted TetCP was detected in S50-6 h at 2θ values of 25.57 and possibly 30°. Slow dissolution of TetCP was previously reported during the formation of pure SHAp from TetCP and DCPA precursors [22]. Unreacted POP was also detected at 2θ values 25.72 and possibly 30°. In fact, the peak at $2\theta = 30$ is controversial between TetCP, POP, and calcium phosphate sulfate hydrate (card # 46-657; shown in the pattern as X). This phase was also detected at 2θ values of 32.08, 29.39, and exclusively at 21.02°. In addition, HAp was detected at 2θ values of 31.92, and 25.9°. No sign of gypsum was found in the XRD pattern of this sample. However, phase assemblage in S50-24 included gypsum as the main phase, followed by hydroxyapatite and calcium phosphate sulfate hydrate. No signs of any of the precursors were found. Gypsum was detected at 2θ values 33.39, 31.15, 29.15, 23.4, and 20.76°, hydroxyapatite was detected at 2θ values 32.81, 32.15, 31.85, and 25.93°, while calcium phosphate sulfate hydrate was detected as 2θ values 34.55, 29.9, and 28.18°. On the JCPDS card of the calcium phosphate sulfate hydrate phase (card # 46-657), it is mentioned that this phase was formed by storing an aqueous solution of pH 5.5 containing $CaCl_2\cdot 2H_2O$, $NH_4H_2PO_4$, $(NH_4)_2HPO_4$, and $Na_2SO_4\cdot 10H_2O$ until complete precipitation of the phase [23]. These salts are all water-soluble, and are therefore considered sources of Ca^{2+}, SO_4^{2-} and PO_4^{3-} ions into solution. It is, therefore, evident that the co-existence of these ions in the current systems resulted in the formation of the same double salt phase; calcium phosphate sulfate hydrate. Its concentration is shown in the XRD pattern of S50-24 h to be lower than that in S50-6 h, suggesting that formation of this phase could be as an intermediate compound before it dissolves into HAp and Gypsum.

In contrast to these findings, the XRD patterns of composites containing 50 wt% of C-SH and S-SH after 1 h of hydration are also shown in Fig. 6. This timing was selected based on the fact those samples showed a relative delay in the growth peaks of gypsum compared to pure gypsum samples. In addition to HAp, POP and gypsum phases, peaks at 36.2, 34.3, 33.25, 32.19, and 30° indicate the possibility of presence of the calcium phosphate sulfate hydrate phase (card # 46-657). This may be related to the slight involvement of the possible non-stoichiometric impurities, in both C-SH and S-SH, in the conversion of POP into gypsum. It should be mentioned, in this regard, that XRD patterns of these composites after 2 h of hydration showed gypsum and HAp as the only phases existing. As was previously stated, conversion of POP into gypsum takes place through a direct dissolution/re-precipitation process. These XRD results, therefore, indicate that the presence of calcium phosphate sulfate hydrate phase (card # 46-657) may only take place when extra calcium and phosphate ions are present in the medium. Moreover, it is also evident that formation of this phase takes place as an intermediate that later converts into distinct hydroxyapatite and gypsum phases. It should be mentioned that XRD patterns of solids separated after 24 h of hydration revealed the presence of the final products only, where neither the starting nor the intermediate phases were found.

Fig. 7A shows the IR spectra of solids obtained after 24 h of hydration of composites containing SHAp and POP precursors, compared to that of as-received gypsum powder. Gypsum is characterized by its bands at 601, 669, 1100.9, 1184, 1624.5,

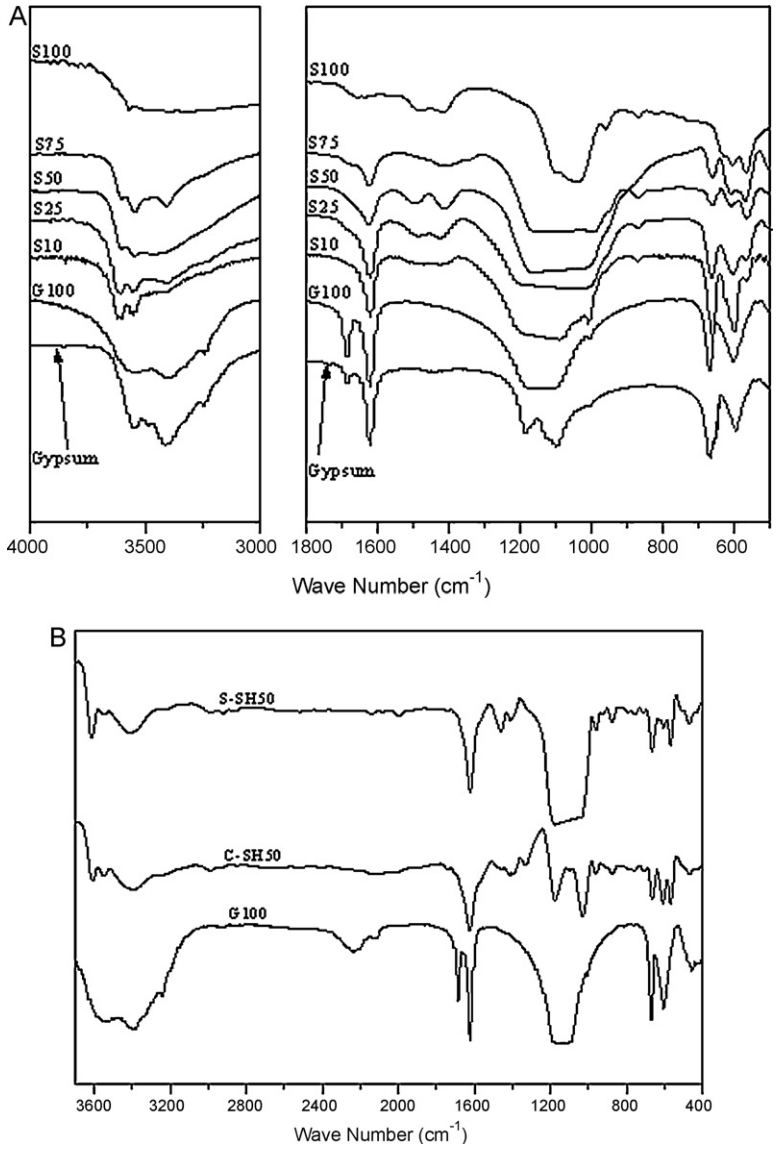

Fig. 7. (A) Infrared spectra of composite powders containing 10, 25, 50 and 75 wt% of SHAp with gypsum after hydration in de-ionized water for 24 h at 37.4 °C. Spectra of pure SHAp (SHAp100) and gypsum (G100) are also shown for comparison. (B) Infrared spectra of composite powders containing 50 wt% of S-SH and C-SH with gypsum after hydration in de-ionized water for 24 h at 37.4 °C. A spectrum of pure gypsum (G100) is also shown for comparison.

1685.8, 3408.5 and 3548 cm^{-1} [24]. Pure gypsum formed in the current study showed a matched spectrum with the two bands at 1100.9, 1184 cm^{-1} fused in a broad band with maxima extending between 1099.3 and 1180.9 cm^{-1}. Broadness of this band increased as the concentration of SHAp increased in the composite to span between 990 and 1200 cm^{-1} in order to accommodate the apatitic phosphate absorption band between 990 and 1104 cm^{-1}. Moreover, the gypsum bands decreased in intensity as the concentration of gypsum in the composites was decreased. Two apatitic bands at 566 and 611 cm^{-1} started to develop and increase in intensity as the concentration of SHAp was increased. The two broad bands at 3408.5 and 3548 cm^{-1} for gypsum were developed to two medium, sharp bands at 3553.4, and 3609.2 cm^{-1} in addition to one broad band at 3445.5 cm^{-1} with the presence of SHAp in the produced composites. In this area, SHAp is known by a weak, but sharp band at 3500 cm^{-1} [24]. These shifts could be, therefore, attributed to the presence of different types of hydrates in the produced structures since both gypsum and calcium phosphate sulfate hydrate phases are both hydrated in addition to the apatitic hydroxyl groups. Fig. 7B, on the other hand, shows IR spectra of composites containing 50 wt% of both C-SH and S-SH after 1 h of hydration, as compared with that of pure gypsum sample. Bands were found at wave numbers 605.9, 664.9, 1622.9, 3408.7 and 3550 cm^{-1} in addition to a broad main band spanning from 1026.9 to 1187.9 cm^{-1} in the spectrum of S-SH/gypsum. On the other hand, bands at wave numbers of 608.7, 662.1, 1622.9, 3400, and 3550 cm^{-1} in addition to two resolved bands at 1029.7 and 1179.4 cm^{-1} in the spectrum of C-SH/gypsum. The slight shift in almost all bands in both spectra may indicate the incomplete formation of gypsum.

Hydroxyapatite, on the other hands, is known by its bands at 566, 611, and a broad band at 990–1070 cm^{-1}. Two bands were

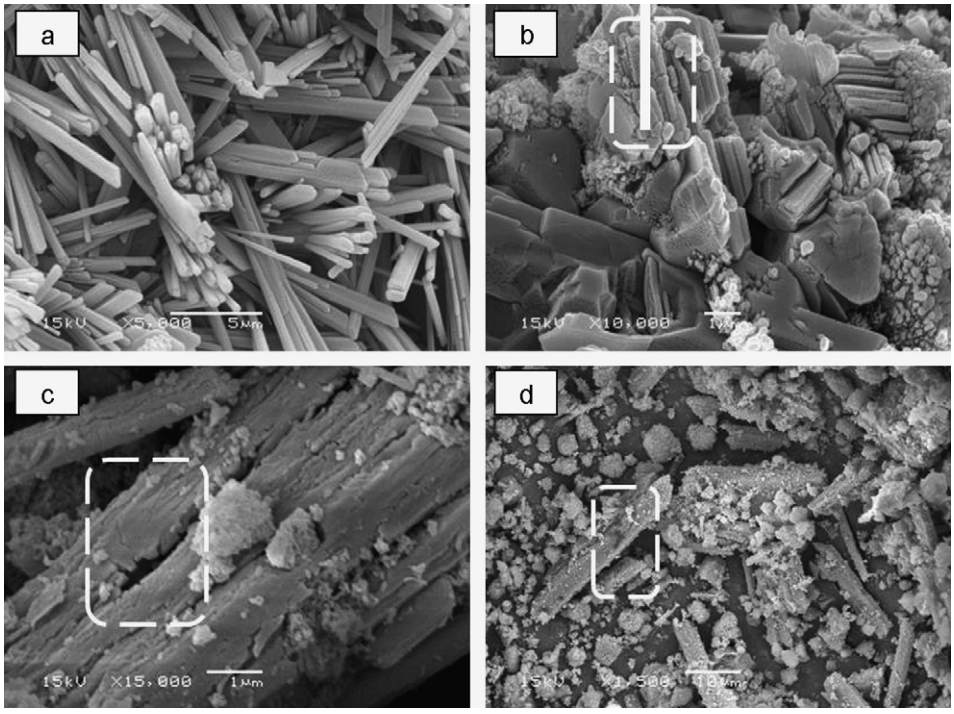

Fig. 8. SEM micrographs of composite powders containing (A) 0, and 50 wt% of (B) SHAp, (C) C-SH, and (D) S-SH with gypsum after hydration in de-ionized water for 6 h at 37.4 °C.

shown at 565.9, and 1029 cm^{-1} were shown in the spectrum of C-SH/gypsum composite, and two corresponding bands at 568.7 and 1026 cm^{-1} were observed in the spectrum of S-SH/gypsum composite. Moreover, a sharp band was observed at 3609.7 and 3615.4 cm^{-1} in the C-SH/gypsum and S-SH/gypsum samples, respectively. This may be attributed to the absorption of the apatitic –OH group.

Fig. 8 shows SEM micrographs of the set gypsum cement compared with solid powders collected from suspensions containing 50 wt% of SHAp, C-SH and S-SH after 6 h of hydration. Gypsum is characterized by its elongated needle-shape crystals with homogeneous size distribution and an average fiber size of 15 μm; Fig. 8A. Fig. 8B shows the interlocking between the deposited irregular-shaped SHAp crystals and the gypsum. However, signs of deformation of the gypsum crystals were found; shown as dotted square in Fig. 8B, which is different from the smooth gypsum crystals shown in Fig. 8A. This could be attributed to the effect of presence of calcium phosphate precursors on the growth kinetics of gypsum, which was previously proven. This phenomenon was also observed in the micrograph of C-SH50 and S-SH50 powders. These results, therefore, confirm the above findings where delayed growth of gypsum crystals causes its deformation.

4. Conclusions

The formation of gypsum in the presence of three types of stoichiometric hydroxyapatites, with different origins, was studied. The *in situ* formation of SHAp via the dissolution/re-precipitation of its precursors was found to affect the growth kinetics of gypsum from its precursors. A delay in the formation of gypsum, that is known to take place in a fast fashion in pure samples, was observed. On the other hand, a relatively lower retardation effect was observed in the presence of ready-made commercial apatite, and was attributed to the possibility of presence of non-stoichiometric apatitic impurities with the commercial product. The presence of read-made synthetic apatite was found to minimize the heat evolution during the formation of gypsum without affecting the growth kinetics of the later. Variations in the pH of the studied solutions showed the effect of POP on decreasing the alkalinity of the media containing SHAp precursors. The presence of C-SH and S-SH were shown to bring pH of the media involving their composites with POP to near physiologic regimes. Evaluation of the phase composition of the formed composites at various time periods during their formation revealed the possibility of the formation of a calcium sulfate-phosphate double salt as an intermediate phase. The current results concludes that novel bone cements could be prepared using calcium phosphates of different origins where the proportions of the apatitic component of the cement are to be dictated by properties of the prepared cements, which are currently being evaluated.

Acknowledgements

This work was partially funded by the Research Affairs of the United Arab Emirates University; project #02-03-2-11/06.

References

[1] B. Flautre, J. Lemâitre, C. Maynou, P. Van Landuyt, P. Hardouin, J. Biomed. Mater. Res. 66A (2003) 214–223.
[2] M. Ikenaga, P. Hardouin, J. Lemâitre, H. Andrianjatovo, B. Flautre, J. Biomed. Mater. Res 40 (1998) 139–144.

[3] J. Barralet, L. Grover, U. Gbureck, Biomaterials 25 (2004) 2197–2203.
[4] H. Monma, T. Kanazawa, J. Ceram. Soc. Jpn. 108 (2000) S75–S80.
[5] Y. Greish, P. Brown, J. Biomed, Mater. Res. B: Appl. Biomater. 67B (2003) 632–637.
[6] G. Orsini, J. Ricci, A. Scarano, G. Pecora, G. Petrone, G. Lezzi, J. Biomed. Mater. Res. B: Appl. Biomater. 68B (2004) 199–208.
[7] P. Maragos, N.F. Bissada, R. Wang, R.P. Cole, Int. J. Periodont. Rest. Dent. 22 (2002) 493–501.
[8] J. Lemâitre, E. Munting, A. Mirtchi, Stomato 91 (1991) 1–5.
[9] C.K. Kim, H.Y. Kim, J.K. Chai, K.S. Cho, I.S. Moon, S.H. Choi, J.S. Sottosanti, U.M. Wikesjo, J. Periodont. 69 (1998) 982–988.
[10] G.E. Pexcora, D. DeLeonardis, C.D. Rocca, R. Cornelini, C. Cortesini, Int. J. Oral. Max. Imp. 13 (1998) 866–873.
[11] M.H. Bai, X.Y. Liu, B.F. Ge, C. Yallg, D.A. Chen, Int. Surg. 81 (1996) 390–392.
[12] E. Fernández, M. Vlad, M. Gel, J. López, R. Torres, J. Cauich, M. Bohner, Biomaterials 26 (2005) 3395–3404.
[13] M. Nilsson, E. Fernandez, S. Sarda, L. Lidgren, J.A. Planell, J. Biomed. Mater. Res. 68B (2002) 199–208.
[14] M. Bohner, Biomaterials 61 (2004) 600–607.
[15] S. Sato, T. Koshino, T. Saito, Biomaterials 19 (1998) 1895–1900.
[16] P.A. Glazer, U.M. Spencer, R.N. Alkalay, J. Schwardt, Spine J. 1 (2001) 395–401.
[17] Y.E. Greish, Egyp. J. Chem. 22 (2007) 2728–2734.
[18] E.J. Prosen, P.W. Brwon, F.L. Davies, Cem. Concr. Res. 15 (1985) 703.
[19] R.I. Martin, P.W. Brown, J. Biomed. Mater. Res. 35 (1997) 299–308.
[20] W.E. Brown, L.C. Chow, A New Calcium Phosphate, Water-setting Cement, American Ceramic Society, Westerville, 1987.
[21] P.W. Brown, N. Hocker, S. Hoyle, J. Am. Ceram. Soc. 74 (1991) 1848–1854.
[22] K.S. TenHuisen, P.W. Brown, J. Biomed. Mater. Res. 36 (1997) 233–241.
[23] Powder Diffraction File 4, Set 56, International Centre for Diffraction Data, Newtown Square, PA, 2006.
[24] J.A. Gadsden, Infrared Spectra of Minerals and Related Inorganic Compounds, Butterworth group, USA, 1975.